RaINS and HEC-HMS Applications for Flood Nowcasting in the Langat River Basin

Wardah Tahir[1,*], Noor Shazwani Osman[1], Jazuri Abdullah[1], Muhammad Azizi Mohd Ariffin[2], Hafiz Hassan[3], Lariyah Mohd Sidek[4], Hidayah Basri[5], Suzana Ramli[1], Nursalleh K Chang[6], and Yip Weng Sang[6]

[1]Faculty of Civil Engineering, Universiti Teknologi MARA Shah Alam, Selangor, Malaysia
[2]Faculty of Computer and Mathematical Sciences, Universiti Teknologi MARA, Shah Alam, Malaysia
[3]Department of Irrigation and Drainage, Kuala Lumpur 50626 Malaysia
[4]ZHL Engineers Sdn Bhd Seri Kembangan, Selangor 43300 Malaysia
[5]Dam Safety Management & Engineering Group, Institute of Energy Infrastructure, Universiti Tenaga Nasional
[6] Malaysian Meteorological Department, Petaling Jaya, Selangor, Malaysia
Email: warda053@uitm.edu.my (W.T.); 2021419378@student.uitm.edu.my (N.S.O.); jazuri9170@uitm.edu.my (J.A.); azizi.ariffin@uitm.edu.my (M.A.M.A.); hafizhassan@water.gov.my (H.H.); lariyah@uniten.edu.my (L.M.S.); bhidayah@uniten.edu.my (H.B.); suzana799@uitm.edu.my (S.R.); nursalleh@met.gov.my (N.K.C.); yipws@met.gov.my (Y.W.S.)
[*]Corresponding author

Manuscript received December 8, 2024; revised January 23, 2025; accepted April 9, 2025; published September 19, 2025

***Abstract*—Floods are one of the most prevalent natural disasters in the world, posing substantial hazards to human life and causing extensive property damage. Reliable flood forecasting enables timelier flood rescue and evacuation, resulting in fewer socioeconomic losses. Despite improvements, existing flood forecasting systems lack the reliability required for practical use in real-world scenarios. Inaccurate forecasting can erode public trust, which may reduce the possibility that people will follow warnings in the future. This paper describes the application of the Radar Integrated Nowcasting System (RaINS) to produce 3h, 2h, and 1h calibrated Quantitative Precipitation Nowcast (QPN) data for input to flood forecasting. The radar QPN is used as alternative rainfall input to the hydrological model in HEC-HMS software to simulate an extreme flood event over the Langat River basin, Malaysia. RaINS data combine radar advection adopting SWIRLS (Short-range Warning of Intense Rainstorms in Localized Systems) with the Numerical Weather Prediction (NWP) model. The results indicate that the radar Quantitative Precipitation Estimate (QPE) from RaINS can perform very well and is slightly better than the raingauge value in simulating the flood, with an NSE value of 0.77 for the raingauge estimation and 0.78 for the RaINS QPE. However, the QPN data have not performed as accurately as the QPE, especially for the 2h and 3h lead times. Nonetheless, although not quantitatively precise, the simulation results indicate that the QPN data can provide an early approximation of the impending flood disaster. Integrating QPN derived from the RaINS data with the HEC-HMS model can provide a flood nowcasting system with an extended lead time for timely warnings and rescue operations. The simulated case study is scalable to other regions. Further research is recommended to enhance the reliability of the QPN and the integrated flood nowcasting system.**

***Keywords*—flood nowcasting, RaINS, Langat River Basin, mean bias correction, radar rainfall, Quantitative Precipitation Estimates (QPE), Quantitative Precipitation Nowcast (QPN)**

I. Introduction

Floods are one of the most frequent natural disasters in the world, posing significant risks to human life and resulting in extensive property destruction [1, 2]. Climate change and urbanization have exacerbated the flood control crisis [3]. Every year, flooding causes an estimated $300 billion in damage and societal impact, prompting experts around the world to address the issue with increased diligence [4]. In 2011, the Thailand flood resulted in $48 billion in damages and displaced 5 million people [5]. The flood disaster that devastated Malaysia in December 2021 claimed roughly 50 fatalities and displaced over 40,000 people, with total damages of approximately RM6.1 billion, with Selangor being the worst affected state [6]. Normally, during the end of the year, the northeast monsoon, where cold northeasterly winds carry moisture-laden air across the South China Sea, often causes severe flooding to the eastern coast of Peninsular Malaysia. However, this time the combined presence of Typhoon Rai and Tropical Depression 29W had intensified the effects of the monsoon, allowing a substantial amount of rainfall to outspread to the western and central parts of Peninsular Malaysia [7]. It was also recorded by Public Infobanjir that some rainfall stations recorded an amount of rainfall up to 380 mm in a day, which is more than the average monthly rainfall in Malaysia of 252 mm. The quick-rising floodwater unexpectedly inundated the properties of the flood victims. Rivers and channels overflowed in the cities, cutting off main roads and submerging hundreds of cars in the floodwater. The disaster was extraordinary, and the victims expressed their dissatisfaction over the lack of warning about the imminent disaster. The recent flood disaster indicates reliable forecasts are crucial for early warning in order to reduce the damages caused.

The existing flood forecasting systems, despite their attempts, lack the necessary reliability for practical application in real-world scenarios [8]. Due to the numerous sources of uncertainty in the underlying flood simulation modelling [9], minimizing flood forecast uncertainty remains a challenging endeavor. A better scientific understanding of physical events and processes enables us to create more realistic models, improve observational measurements of hydrometeorological variables, and enhance model input prediction [10]. At present, significant advancements in flood modeling and forecasting can be credited to several factors, including the availability of various sophisticated 3-D hydrodynamic modeling software and the increased accessibility of high-performance computers that possess superior processing speeds, larger memory capacities, and enhanced data storage capabilities, in addition to the widespread availability of high-resolution geophysical data

sets obtained from remote-sensing sites, which are crucial for accurately estimating and calibrating model parameters. The rapid growth of the Internet and the widespread use of mobile phones have also significantly influenced the dissemination of flood warnings [5].

Flood forecasting systems worldwide combine meteorological, hydrological, and hydraulic models to forecast floods and provide early warnings. In Malaysia, the National Flood Forecasting and Warning System (NaFFWS) uses real-time rainfall data, river flow information, and weather prediction to issue alerts. Despite their advancements, the systems face challenges such as data availability in inaccessible areas, high computational costs, and the need for more accurate real-time monitoring, especially in the face of extreme weather events driven by climate change [6].

To accurately forecast hydrologic responses at longer lead times, it is necessary to use precipitation amounts at future time steps known as quantitative precipitation forecasts (QPFs). The quantitative precipitation forecast (QPF) integration is essential for extending the lead time for flood warnings in small and medium-sized urban river basins due to the short response time of the basin [11, 12]. Over several decades, researchers have devised various methodologies for the short-term QPF. The highly variable complexity of tropical localized rainfall patterns, both spatially and temporally, poses a great challenge in forecasting them.

This study aimed to improve the accuracy of the flood forecasting system by employing the quantitative precipitation nowcasts (QPN) from the RaINS data. The acronym 'QPN' was used instead of QPF to indicate the very short-term (3, 2, 1h) forecast. Additionally, the term 'flood nowcasting' is used to refer to short-term forecasting.

The paper describes an integrated hydro-meteorological flood model using Radar Integrated Nowcasting Systems (RaINS) data, which blends radar data from SWIRLS (Short-range Warning of Intense Rainstorms in Localized Systems) with numerical weather prediction (NWP) model products. Radar echoes advection to predict the rainfall and are found to have more skill over time scales of several hours compared to NWP. However, over longer time scales where the larger dynamical flows are better resolved by the NWP, it overtakes the skill of nowcast. To leverage the strengths of both nowcasting techniques, the RaINS framework integrates the SWIRLS methodology with the NWP approach. The novelty of this paper lies in the derivation of calibrated quantitative precipitation nowcast (QPN) from the RaINS to forecast extreme rainfall events and integrate this data into an HEC-HMS river basin model for flood forecasting. The integration of the calibrated pixel-based radar QPN with the lump hydrological model introduces a new approach to the data input algorithm, which has a moderate processing time for flood modeling.

II. Literature Review

Many studies have used radar rainfall as an input for flood forecasting [13–20]. Knebl *et al*. [21] developed a framework for a flood forecasting system at the San Antonio River Basin using NEXRAD rainfall radar data with 4×4 km resolution as rainfall input data into a gridded basin in the HEC-HMS model. Smith *et al*. [22] studied flash flood forecasting by using radar rainfall estimation in small urban watersheds. Radar rainfall estimation was derived based on the power law method (Z-R relationship), and a rain gauge network was used to examine the bias of radar rainfall estimates. Meanwhile, Sharif *et al*. [23] postulated that flood forecasting in urban areas requires distributed precipitation estimates provided by radar and a distributed hydrologic model. Sun *et al*. [24] used radar rainfall data via the window probability matching method (WPMM) and utilized the cokriging of rain gauge and radar rainfall data for flood estimation studies. Generally, radar data has the advantage of superior spatial distribution of the precipitation field compared to rain gauges, but quantitative precipitation estimates (QPEs) directly derived from radar reflectivity measurements are subject to errors and uncertainties. Various techniques have been developed for real-time correction of systematic biases in radar precipitation fields by adjusting radar precipitation to rain gauge measurements [25–31].

Previous studies indicate the most encouraging approach for developing QPFs with useful lead times is by combining NWP model forecasts with blends of extrapolated patterns of radar or satellite and gauged rainfall data. For example, the UK Met Office combined radar advection with NWP-based QPF using relative weights [32] in the operational NIMROD system [33] designed for 1–6 h QPF. The Advanced Regional Prediction System (ARPS) storm-scale NWP developed by the University of Oklahoma and radar observation were blended to forecast severe storms in Oklahoma with high spatial resolution of 0.01°×0.01° (~1 km×1 km) and 1-minute intervals. Multi-Scale Tracking and Forecasting Radar Echoes (MTaRE) was used to evaluate the accuracy of forecasts. It was found that the MTaRE model performance decreased rapidly with lead times since radar-based extrapolation ignored the temporal evolution of storms, while the ARPS model was able to forecast the evolution but overestimated the storms. An ensemble of radar rainfall forecasts from a stochastic advection-based scheme was generated and later improved as the Short-Term Ensemble Prediction System (STEPS), which merges with downscaled NWP model forecasts [34]. Other merged NWP and radar projects for optimal predictions include GANDOLF (Generating Advanced Nowcast for Deployment in Operational Land Surface Flood Forecast) (Pierce *et al.* 2000) and RAPIDS (Rainstorm Analysis and Prediction Integrated Data-processing System) [35].

III. Materials and Methods

The section provides background information on RaINS data, the case study area, QPN calibration, and the integration of QPN data with the HEC-HMS model for flood modeling.

A. RaINS Data

RaINS utilizes SWIRLS, which adopts the concept of pure advection of radar echoes for short-range precipitation nowcasting. It employs a backward semi-Lagrangian scheme to project radar echoes using optical flow velocity. Inverse distance weighted (IDW) interpolation is used to interpolate the radar data grid from 18 individual stations. Subsequently, only the maximum grid value is chosen from the interpolated

individual radar data to generate a Malaysian integrated radar grid. An arctangent function is employed to map radar data to grayscale images. This step resolves intense individual echoes and eliminates noise. Next, the radar data undergo further pre-processing (Gaussian smoothing) before using the optical flow scheme to generate the velocity flow field between the radar input data at -10 min and 0 min. Then, a backward semi-Lagrangian advection scheme is used to extrapolate the latest radar reflectivity field up to 3h ahead using the velocity flow field [36].

The NWP blending uses maximum vertical reflectivity produced by the MMD-WRF-ARW forecasts. The forecasts are produced every hour up to 7 days or 137h ahead to provide forecast guidance using GFS 0.25° data as a boundary condition with 3-way nesting (9 km, 3 km, and 1 km). As for the planetary boundary, the Yonsei University Scheme (YSU) is used. The weights of radar extrapolation and NWP should be adjusted because they will change with time. Radar extrapolation should get the maximum weight at the earlier time period of the nowcast, but as the nowcasting extends, the rate of radar extrapolation errors increases; therefore, the NWP products should be given a larger weight to lengthen the nowcast limitation and enhance the nowcast accuracy. Fig. 1 illustrates the nowcast skills for radar extrapolation with NWP blend.

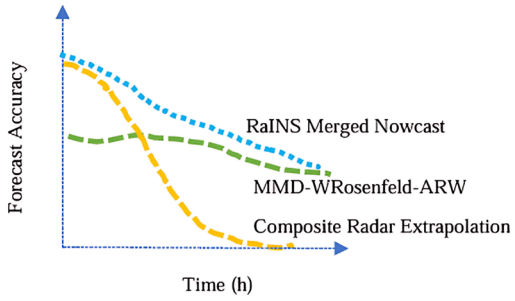

Fig. 1. The forecast performance comparison for RaINS components.

The blending process involves quantile mapping and phase correction to make the NWP image resemble a radar image before the two images are blended to produce RaINS. The NWP grid with 1 km resolution will be combined with a radar grid of 833 m resolution using bilinear interpolation, producing a new grid of 833 m resolution. To get optimal nowcast results, a time-varying function and a hyperbolic tangent function are used. The formula used for these two approaches is shown in Eq. (1) and (2):

$$(t) = g \times a \times \frac{(\beta-\alpha)}{2}[1 + tanh(y(t-9))] \quad (1)$$

$$QPF_{RaINS} = (1 - w(t))1 \times RADAR^{EXTRAPOLATION} + w(t) \times NWP \quad (2)$$

B. Case Study Area

The Langat River basin flows through the Selangor state of Malaysia. The Langat River spans 78 km in length and has a catchment area of 2350 km^2. It starts with Gunung Nuang in the Titiwangsa Range as shown in Fig. 2. It flows in a westerly direction toward the Straits of Malacca. The primary tributaries of the Langat River are the Sungai Semenyih and Sungai Labu.

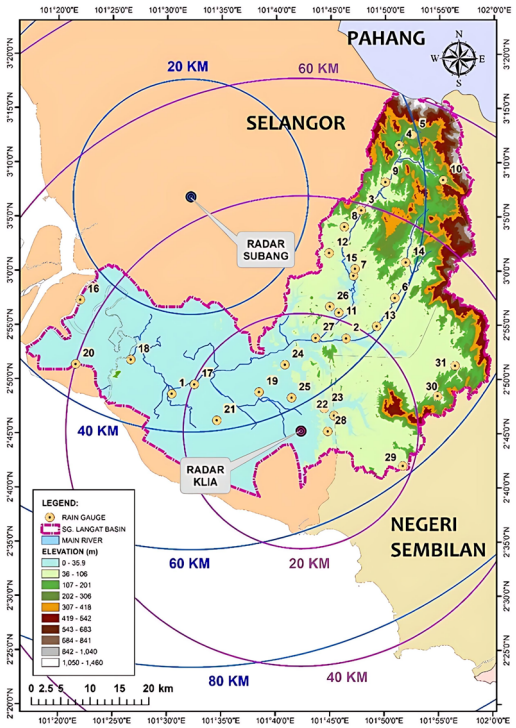

Fig. 2. Langat River basin and the location of rainfall stations.

C. Radar-Gauge Bias Correction

By utilizing rain gauge data, a bias, also called the systematic difference between radar rainfall and rain gauge, can be gradually eliminated; thus, bias correction is introduced [37]. Qiu *et al.* [38] stated that in radar meteorology, Mean Field Bias (MFB) modification or correction is the most common technique, and the correction factor is calculated as the ratio of the cumulative rain gauge rainfall, G, and the accumulated radar rainfall, R. This method removes the bias introduced through the uncertainty in the radar calibration or an erroneous coefficient in the Z-R relationship. MFB assumes that a uniform multiplicative error affects the radar QPEs. Therefore, a single adjustment factor (C_{MFB}) is estimated with the following formula:

$$C_{MFB} = \frac{\sum_{i=1}^{n} G_i}{\sum_{i=1}^{n} R_i} \quad (3)$$

where,

G = gauged rainfall (hourly depth)
R = radar rainfall (hourly depth)
n = number of gauge station involved in calibration

The above formula indicates that n represents the number of the valid rain gauges, Gi is the rain gauge observation, and Ri is the radar-estimated value at the rain gauge-located pixel. MFB is usually applied uniformly to a wide area; it often ignores spatial variability on radar QPEs when used on a small scale [38].

Since a single factor for a large area leads to large errors due to spatially non-uniform rainfall events, we applied creating smaller regions with clusters of rain gauges in determining the MFB correction factor. The smaller regions were delineated based on the analysis of the median of the radar/gauge ratio. Using the available data, the median was determined, isopleths of similar medians were drawn, and clusters of rainfall stations were determined. During the

calibration process, each region would have its unique adjustment factor. A midpoint would be identified in each region, and radar pixels would be multiplied by the mean of the five closest factors for bias adjustment.

The haversine formula was used to determine the closest factors based on midpoint coordinates. The formula is shown as follows:

$$a = \sin^2(\frac{\Delta\varphi}{2}) + \cos\varphi 1.\cos\varphi 2.\sin^2(\frac{\Delta\lambda}{2})$$
$$c = 2.(a\tan 2)(\sqrt{a}, \sqrt{(1-a)}) \quad (4)$$
$$c = R * c$$

where, φ is latitude, λ is longitude, R is earth's radius

(radius = 6,371 km), and the angles need to be in radians to pass to trig functions.

D. RaINS Data Input to HEC-HMS Model Catchment

The HEC-HMS model is frequently used in many hydrological investigations because of its versatility (it can simulate both short- and long-term runoff events) and user-friendliness [39–41]. The available resources for this model include a basin model, metrological model, control specification, and time series data [42]. The meteorological model's inputs were the streamflow and precipitation data. The method of the meteorological model applied in this study was specified by a hyetograph. The control specifications component regulates the simulation period. In this study, the simulation's control specification called for an hourly time step and covered the period from December 16 to 25, 2021. In addition, the model is comprised of subsystems that figure out elements such as base flow, direct runoff, and compute runoff. It was determined using the hourly constant base flow, SCS-CN, SCS-UH, and Muskingum methods. To prepare the input data for the HEC-HMS model, a pre-processing tool called the HEC-GeoHMS extension of ArcGIS was utilized. The hydrologic inputs that constitute the HEC-HMS model require a large number of data sets, any of which can be loaded from HEC-GeoHMS.

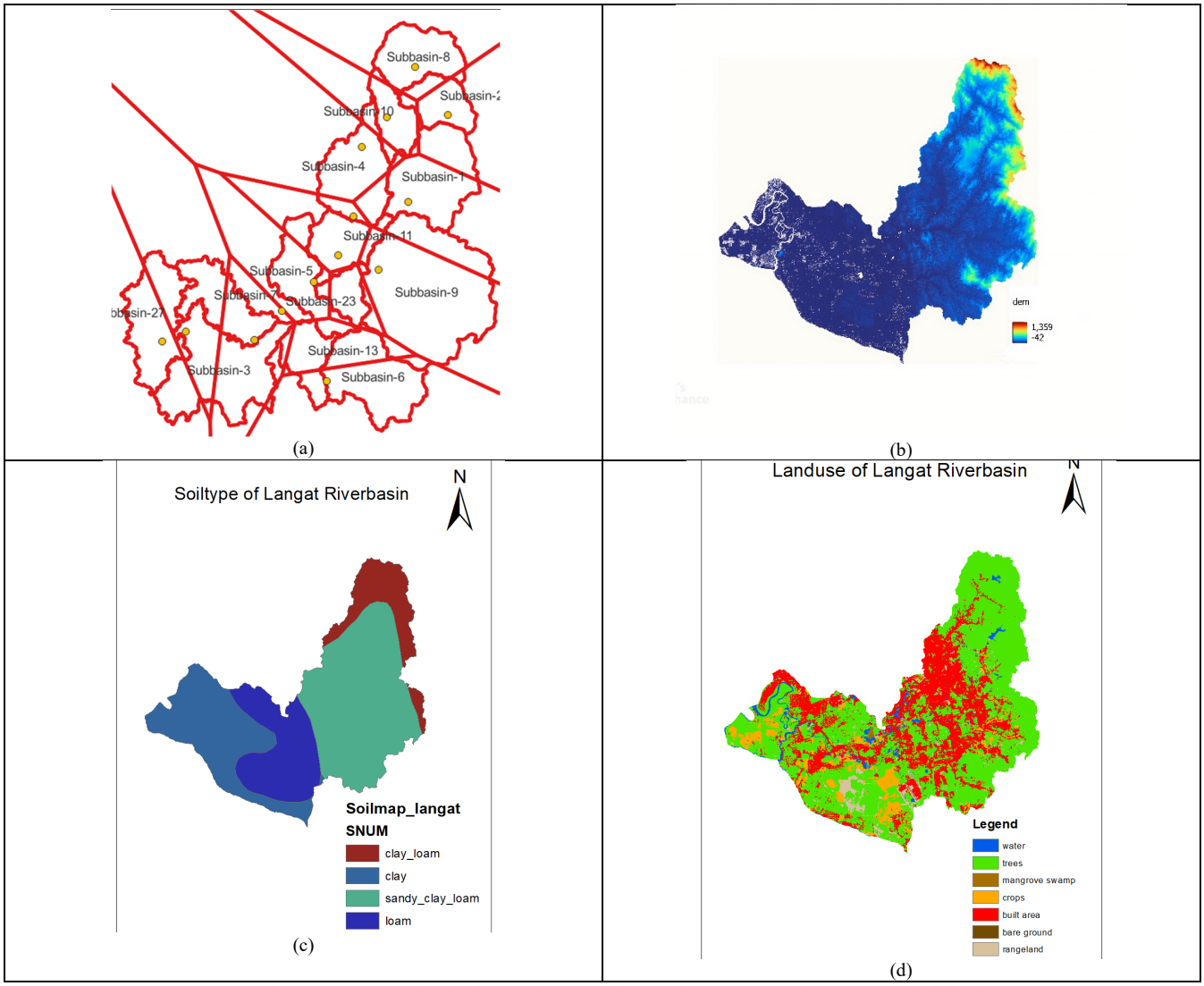

Fig. 3. Data collection of Langat River basin: (a) Thiessen polygon, (b) DEM, (c) soil type map, and (d) land use map.

1) Data input and river basin model development

This study utilized hydrological data, including rainfall and streamflow records provided by the Malaysian Department of Irrigation and Drainage (DID) and QPF derived from the RaINS data. The rainfall pattern in the watershed was spatially diverse, and the Thiessen polygon method was employed to compute the mean rainfall over the catchment depicted in Fig. 3(a). Next, for the topographic map, a Shuttle Radar Topography Mission (SRTM) Global DEM of 30m resolution was acquired from the USGS website, which

included the whole Sungai Langat catchment area, as shown in Fig. 3 (b). The soil type map for the Langat catchment was obtained from the Digital Soil Map of the World (DSMW) and shows three different types of soil in the area: sandy, clay, and loam, as illustrated in Fig. 3 (c). Seven classes of land use maps in the Langat watershed shown in Fig. 3 (d) were acquired from the Land Use and Land Cover (LULC) website. These soil type and land use maps are the datasets used to determine the hydrological and further define the SCS-CN value of a catchment. In this study, the SCS-CN loss method was used to calculate the initial runoff from a particular or designed rainfall. The accumulated rainfall excess is dependent on soil type, land use, cumulative precipitation, and preceding moisture conditions, as determined in Eq. (5) [43].

$$P_e = \frac{(P-I_a)^2}{P-I_a+S} \quad (5)$$

where *Pe*=accumulated precipitation excess at time *t*,
P =accumulated rainfall depth at time *t*,
I_a=the initial abstraction (0.2S),
S =potential maximum retention.

Maximum retention (S) is connected to watershed characteristics (via the dimensionless CN) as Eq. (6):

$$S = 25400 - \frac{254 \times CN}{CN} \quad (6)$$

Furthermore, the SCS Unit Hydrograph (SCS-UH) model was used as the transform method to convert excess precipitation into runoff. This was done in order to get the expected outcome. In this approach, the single input is the lag time (Tlag) which means the time from the excess rainfall center of mass to the hydrograph peak and is determined by concentration time, Tc, as shown in Eq. (7):

$$Tlag = 0.6Tc \quad (7)$$

where the variables *Tlag* and *Tc* represent time intervals measured in minutes.

2) Model calibration and application

A well-calibrated model requires both the hydrological model's technical proficiency and the accuracy of the input data. Initially, the HEC-HMS model for the Sungai Langat basin was manually calibrated by comparing observed streamflow peaks, timing, and discharge volumes. Lag time, curve number, initial abstraction, Muskingum-k, and Muskingum-x were adjusted automatically and manually to complete the procedure. The RaINS gridded pixel-based QPN inputs were subsequently applied to the HEC HMS calibrated model. This is achieved through the utilization of Quantum Geographic Information System (QGIS) software. Firstly, the Langat sub-basin shapefile in HEC-HMS was imported into QGIS, as shown in Fig. 4. Next, the mean value for the gridded pixels for each sub-basin was determined using the zonal statistics menu of the QGIS software. Each sub-basin's radar QPN would then be utilized as input for the HEC HMS model's time series data component.

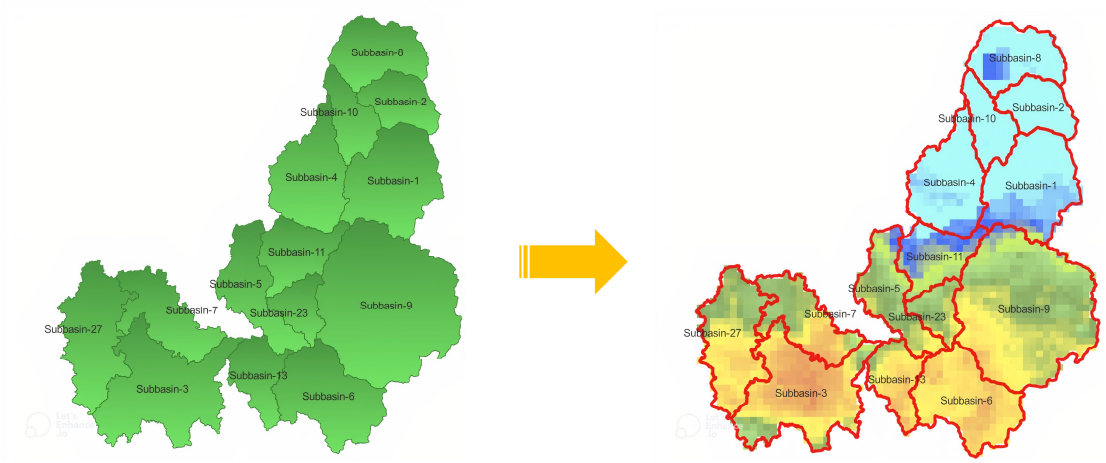

Fig. 4. Mean gridded rainfall by subbasin.

3) Model performance evaluation

The model's performance was then assessed using statistical evaluation approaches, specifically Nash-Sutcliffe Efficiency (NSE) [44] and the root mean square error-standard deviation ratio (RSR).

$$NSE = 1 - \frac{\sum_{k=1}^{M}[(Q_o)_k-(Q_s)_k]^2}{\sum_{k=1}^{M}[(Q_o)_k-\overline{Q_o}]^2} \quad (8)$$

$$RSR = \frac{\sqrt{\sum_{k=1}^{n}[(Q_o)_k-(Q_s)_k]^2}}{\sqrt{\sum_{k=1}^{n}[(Q_o)_k-\overline{Q_o}]^2}} \quad (9)$$

where;
Qo = observed discharge,
Qs = simulated discharge,
$\overline{Q_o}$*= average of observed discharge,*
$\overline{Q_s}$ *=average of simulated discharge,*
M= number of samples.

IV. Result and Discussion

The displays of radar QPN in Fig. 5 demonstrate the performance of the nowcast data. The figures compare 3h, 2h, and 1h nowcast data to actual values at 1800, 1900, and 2000 p.m. on December 17, 2021. The 3-h nowcast figures reveal a reduced distribution of rainfall across the river basin. As the nowcast approaches the actual time, its values improve. It can also be seen that at the third hour of the extreme event (2000 pm), the nowcast values have the lowest relative error, as shown in Table 1. This observation could be attributed to the constant rain pattern throughout the 3h storm event.

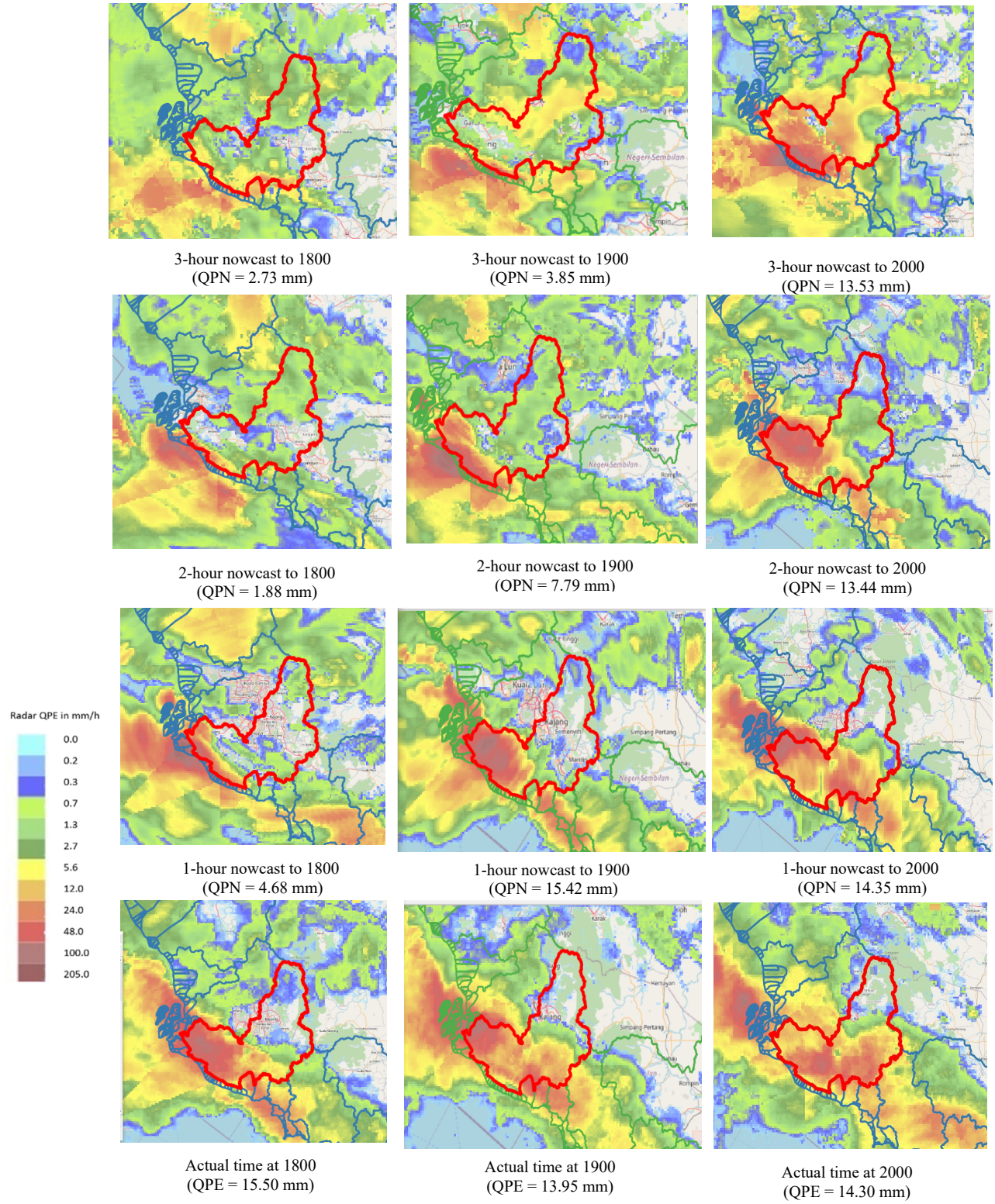

Fig. 5. Mean gridded rainfall by subbasin.

Table 1. Performance comparison between 1, 2, 3-h nowcast of mean areal basin rainfall with the actual recorded value for Langat River basin, 17th. December 2021

Time	Mean Areal Radar QPE (mm)	1-h Nowcast	Relative Error (%)	2-h Nowcast	Relative Error (%)	3-h Nowcast	Relative Error (%)
1800	15.5	4.7	69.8	1.9	87.9	2.7	82.4
1900	14.0	15.4	10.5	7.8	44.2	3.6	74.3
2000	14.3	14.4	0.3	13.4	6.0	13.5	5.4

One obvious benefit of radar data over point gauge rainfall is the ability to see the spatial distribution of rainfall over the catchment on radar displays. As evident from the radar displays, the epicenters of the storm during the December 17, 2021, floods were the lower basin in Kuala Langat and Sepang, which were severely impacted [45]. The nowcast from the RaINS data can provide an early estimate of the upcoming disaster but may not correctly quantify the specific

location and amount of precipitation.

A. RaINS QPN Input to HEC-HMS Model Catchment

The data were imported into HEC-HMS after being pre-processed in ArcMap using the HEC-GeoHMS extension. Fig. 6 (a) presents an illustration of the sub-basins, reaches, and junctions that can be discovered within the research region. The Soil Conservation Service (SCS) CN approach was utilized in this study to calculate infiltration losses. The CN was calculated based on the LULC class and soil type. Fig. 6 (b) shows a spatial representation of the CN grid, indicating that the basin's CN value spanned from 58 to 98. Besides, the SCS approach known as unit hydrograph (UH) was utilized in order to convert excessive precipitation into runoff. Calibration of the model's parameters was accomplished by trial and error. The sensitivity analysis was being carried out to identify the most sensitive parameter. It was discovered that while flood travelling time (k) was more insensitive, Tlag and CN were more sensitive. Changes were made to the range values of each parameter, which varied from +10% to -10%, and this adjustment is considered being acceptable [46].

The efficiency of the model was assessed by comparing observed streamflow to model-simulated values using statistical evaluation criteria such as Nash–Sutcliffe efficiency (NSE) and root mean square error-standard deviation ratio (RSR).

As shown in Table 2, following optimization by using the objective function root mean square error, better results were found between the simulated and actual values based on the Nash-Sutcliffe Efficiency (NSE) criteria. The model performed satisfactorily, with an NSE value of 0.77 for rain gauge estimation and 0.78 for RaINS QPE. In this case study, the RaINS QPN of the 1-hour nowcast was more precise, as the NSE value was 0.82 compared to the 2-h nowcast (0.09) and 3-h nowcast (-0.14). According to Moriasi *et al.* [47], if the Nash-Sutcliffe efficiency of the model simulation is more than 0.5, it is considered satisfactory; if it is more than 0.65, it is considered good; and if it is more than 0.75, it is considered very good. An NSE value of 1 represents a model that predicts perfectly.

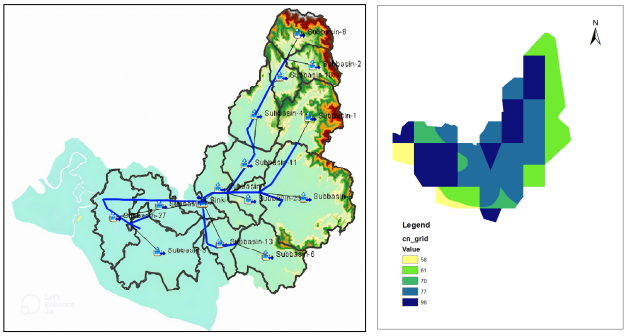

(a) (b)

Fig. 6. (a) HEC-HMS sub-basins schematic diagram, (b) CN value grid map.

Table 2. Simulation and performance result after model calibration

	Total volume (per area) (mm)			Peak discharge (m^3/s)			NSE	RSR
	Simulated	Observed	RE	Simulated	Observed	RE		
Rain gauge	85.6	92.8	7.2	666.4	643.2	-23.2	0.77	0.5
Current Time (radar QPE)	73.9	92.8	18.9	619.7	643.2	23.5	0.78	0.5
1 h _nowcast	74.9	92.8	17.9	632.9	643.2	10.3	0.82	0.4
2 h _nowcast	44.1	92.8	48.7	422.3	643.2	220.9	0.09	1.0
3 h _nowcast	38.0	92.8	54.8	327.7	643.2	315.5	-0.14	1.1

RE: relative error; NSE: Sutcliffe Efficiency; RSR: Root mean square error-standard deviation ratio

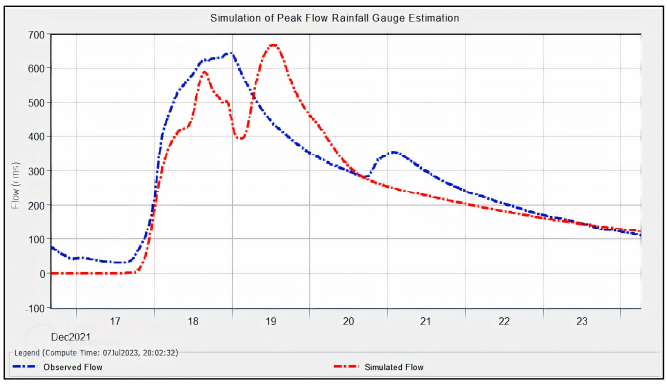

(a)

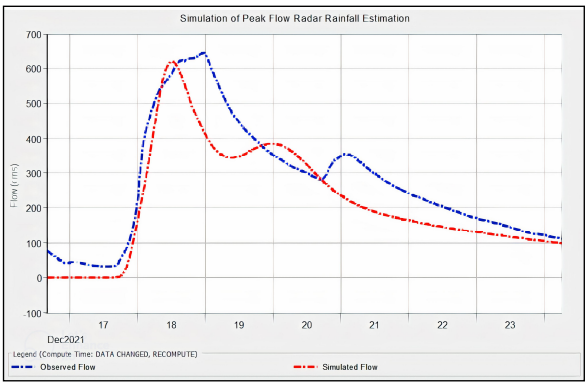

(b)

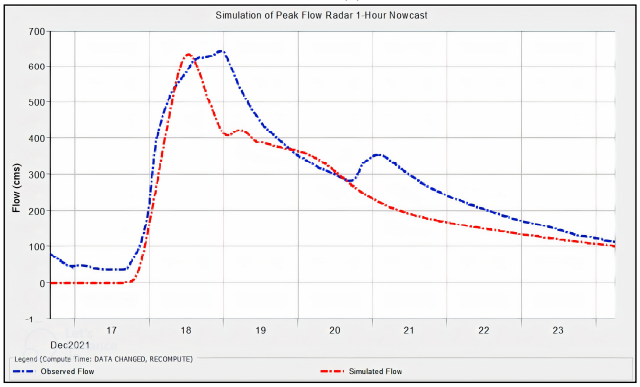

(c)

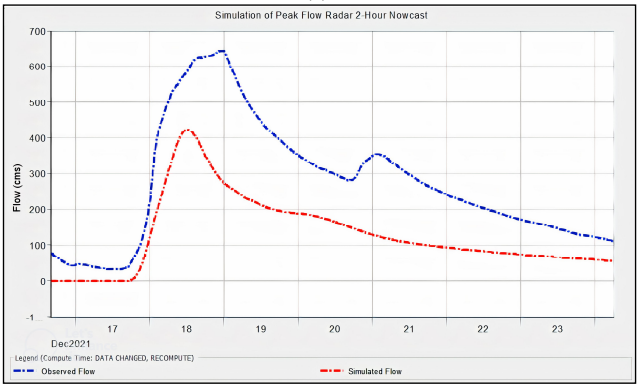

(d)

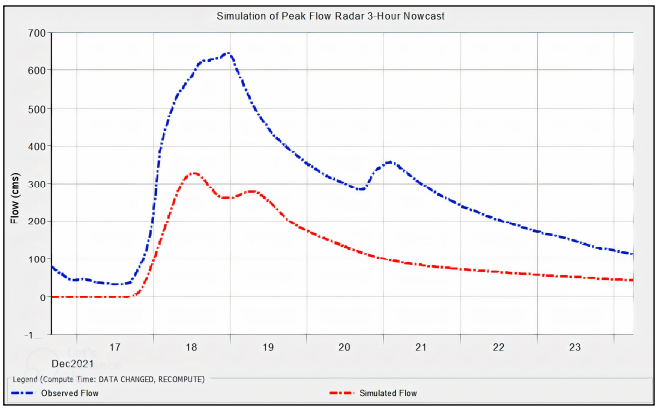

(e)

Fig. 7. Simulated and observed hydrographs output from HEC-HMS using rainfall input from (a) gauge rainfall (b) radar current time (QPE) (c) 1h radar QPN (d) 2h radar QPN (e) 3h nowcast radar QPN.

In addition, the simulation performance of RaINS QPN for a 1-hour nowcast was somewhat better than RaINS QPE when measured by the ratio of the standard deviation of observations to the root mean square error (RSR) value. According to Bárdossy & Pegram [48], the model can be deemed suitable if RSR is less than 0.7.

Fig. 7 demonstrates the simulated outputs from the calibration for rain gauge data, RaINS QPE, and QPN, respectively. The blue line represents the streamflow data obtained at the Dengkil station, while the red line represents the flow that the model generated. In each rainfall estimation, the hydrograph shape was accurately reproduced in the model output. Specifically, the shape of the hydrograph and its peak time matched well. The runoff simulation by rain gauge shows the computed volume was 85.6 mm, which was underestimated to the observed volume (92.8 mm) with a relative error of 7.2%, as depicted in Fig. 7(a). It can also be seen that the observed peak discharge on December 18, 2021, was slightly underestimated compared to the computed peak discharge. Besides, Fig. 7(b) shows the computed volume discharged by RaINS QPE (73.9 mm) resulted in a slightly lower volume than the observed volume (92.8 mm). The peak discharge that was simulated (619.7 mm^3/s) on December 18, 2021, was underestimated compared to the observed peak discharge (643.2 mm^3/s), with a relative error of 23.5%.

Fig. 7(c)–(e) illustrates the rainfall-runoff simulation result for RaINS QPN. As can be seen in the figures, the 1-h nowcast simulated hydrograph captured the observed data more precisely than the 2- and 3-h nowcast model outputs. Nevertheless, these three models adhere to the observed patterns. These simulated hydrographs showed that this HEC-HMS model successfully captured the peak discharge by considering the distributed-mode spatial variability of meteorological factors. The runoff volume simulated using the nowcast data showed less value, though the patterns were approximately similar.

The study showed that the QPN derived from the RaINS data, which blends NWP and radar advection, requires further enhancement, especially in radar advection skills during intense rainfall events, as seen in the case study. Although the NWP-based QPF data performed better than radar-based extrapolation methods over longer time scales, they were sensitive to the initial condition, spatial resolution, and assimilation data, thus lacking in prediction skill in the first short-term [49–51]. Extrapolating radar data can add extra lead time in short-term flood forecasting; however, the predictive accuracy of radar-based extrapolation decreases within the first several hours of severe weather development [49]. This study indicated that the QPN performed very well spatially and temporally during the first hour of the nowcast but became less accurate afterwards. Further research is needed to improve the radar advection's extrapolation abilities when blended with the NWP.

V. Conclusion

This paper describes the application of RaINS to produce 3h, 2h, and 1h calibrated Quantitative Precipitation Nowcasts (QPN). The calibration of the QPN was performed using the mean field bias correction technique with regionalization of the adjustment factor. It was found that the calibrated QPN generated from the RaINS data can offer an initial prediction of an impending flood disaster, but it may not accurately determine the precise location and quantity of precipitation. Next, the QPN values were used as input to the HEC-HMS basin model to simulate an extreme flood event over the Langat River basin, Malaysia. The study introduced a novel method for integrating the radar QPN data with the HEC-HMS model as mean gridded pixel sub-basin values. The simulation results indicate that radar QPE from RaINS performed slightly better than the rain gauge value in simulating the flood. However, the nowcast data may require further enhancement to achieve accuracy comparable to that of the QPE data. The nowcast data, however, can offer an early approximation of the looming flood catastrophe. The integrated system offers a significant improvement to the flood nowcasting system in Malaysia and is adaptable to other regions.

Conflict of Interest

The authors declare no conflict of interest.

Author Contributions

Material preparation, as well as data collection and analysis were performed by W.T., N.S.O., J.A., and M.A.M.A.; H.H., L.M.S., H.B., and S.R. contributed to the revision and improvement of the paper; H.H., N.K.C., and Y.W.S. contributed to the data provider and analyzer; and all authors had approved the final version.

Funding

The authors gratefully acknowledge the Ministry of Higher

Education (MOHE) for funding under the Fundamental Research Grant Scheme (FRGS/1/2021/TK0/UiTM/01/1). This research work is also supported by the Asia-Pacific Network Collaborative Regional Research Program (APN-CRRP) Project (CRRP2022-07MY-Basri) (in which the methodology is applied).

ACKNOWLEDGMENT

We would like to express our gratitude to the Drainage and Irrigation Department and the Malaysian Meteorological Department for their support and for providing the data used in this research.

REFERENCES

[1] F. Zheng, H. Yin, Y. Ma, H. F. Duan, H. Gupta, D. Savic, and Z. Kapelan, "Towards improved real-time rainfall intensity estimation using video surveillance cameras," *Water Resources Research*, e2023WR034831, 2023.

[2] E. Yildirim and I. Demir, "Agricultural flood vulnerability assessment and risk quantification in Iowa," *Science of The Total Environment*, vol. 826, 154165, 2022.

[3] C. Songchon, G. Wright, and L. Beevers, "The use of crowdsourced social media data to improve flood forecasting," *Journal of Hydrology*, 129703, 2023.

[4] P. Weng, Y. Tian, Y. Liu, and Y. Zheng, "Time-series generative adversarial networks for flood forecasting," *Journal of Hydrology*, vol. 622, 129702, 2023.

[5] T. E. Adams and T. C. Pagano, *Flood Forecasting: A Global Perspective*, Academic Press, 2016.

[6] S. Tasnim, S. Aripin, and N. Asif, "Understanding Flood Vulnerability Issues in Hulu Langat Residential Zone: A Study of Taman Sri Nanding, Hulu Langat, Malaysia," *Journal of Advancement in Environmental Solution and Resource Recovery*, vol. 2, no. 2, pp. 56–63, 2022.

[7] S. Rahman, *Malaysia's Floods of December 2021: Can Future Disasters be Avoided?* ISEAS-Yusof Ishak Institute, 2022.

[8] M. Muste, D. Kim, and K. Kim, "A flood-crest forecast prototype for river floods using only in-stream measurements," *Communications Earth & Environment*, vol. 3, no. 1, p. 78, 2022.

[9] J. Abdullah, N. S. Muhammad, and P. Y. Julien, "Envelope curves for the specific discharge of extreme floods in Malaysia," *Journal of Hydro-Environment Research*, vol. 25, pp. 1–11, 2019.

[10] J. D. Salas, G. Gavilan, F. R. Salas, P. Y. Julien, and J. Abdullah, "CHAPTER 28: Uncertainty of the PMP and PMF," in *Handbook of Engineering Hydrology: Modeling, Climate Change, and Variability*, S. Eslamian (Ed.), CRC Press, 2014, ISBN 978146655246.

[11] E. Toth, A. Brath, and A. Montanari, "Comparison of short-term rainfall prediction models for real-time flood forecasting," *Journal of Hydrology*, vol. 239, no. 1–4, pp. 132–147, 2000.

[12] W. Yu, E. Nakakita, S. Kim, and K. Yamaguchi, "Improvement of rainfall and flood forecasts by blending ensemble NWP rainfall with radar prediction considering orographic rainfall," *Journal of Hydrology*, vol. 51, pp. 494–507, 2015.

[13] B. C. Hoblit and D. C. Curtis, "Integrating radar rainfall estimates with digital elevation models and land use data to create an accurate hydrologic model," in *Proc. Floodplain Management Association Spring 2001 Conference*, 2001, pp. 1–9.

[14] T. Wardah, R. Suzana, and S. S. N. Huda, "Multi-sensor data inputs rainfall estimation for flood simulation and forecasting," in *Proc. 2012 IEEE Colloquium on Humanities, Science and Engineering (CHUSER)*, 2012, pp. 374–379.

[15] A. Berne and W. F. Krajewski, "Radar for hydrology: Unfulfilled promise or unrecognized potential?" *Advances in Water Resources*, vol. 51, pp. 357–366, 2013.

[16] D. B. Wright, J. A. Smith, G. Villarini, and M. L. Baeck, "Estimating the frequency of extreme rainfall using weather radar and stochastic storm transposition," *Journal of Hydrology*, vol. 488, pp. 150–165, 2013.

[17] V. Conde, G. Nico, P. Mateus, J. Catalão, A. Kontu, and M. Gritsevich, "On the estimation of temporal changes of snow water equivalent by spaceborne SAR interferometry: A new application for the Sentinel-1 mission," *Journal of Hydrology and Hydromechanics*, 2019.

[18] T. M. Modrick, K. P. Georgakakos, E. Shamir, and C. R. Spencer, "Operational quality control and enhancement of radar data to support regional flash flood warning systems," *Journal of Hydrologic Engineering*, vol. 22, no. 5, E4016001, 2017.

[19] J. Li, L. Li, T. Zhang, H. Xing *et al.*, "Flood forecasting based on radar precipitation nowcasting using U-net and its improved models," *Journal of Hydrology*, 130871, 2024.

[20] S. Ramli, W. Tahir, J. Abdullah, J. Jani, S. Ramli, and A. Asmat, "Flood estimation for SMART control operation using integrated radar rainfall input with the HEC-HMS model," *Water Resources Management*, doi: org/10.1007/s11269-020-02595-4, 2020

[21] M. R. Knebl, Z. L. Yang, K. Hutchison, and D. R. Maidment, "Regional scale flood modeling using NEXRAD rainfall, GIS, and HEC-HMS/RAS: A case study for the San Antonio River Basin Summer 2002 storm event," *Journal of Environmental Management*, vol. 75, no. 4, pp. 325–336, 2005.

[22] J. A. Smith, M. L. Baeck, K. L. Meierdiercks, A. J. Miller, and W. F. Krajewski, "Radar rainfall estimation for flash flood forecasting in small urban watersheds," *Advances in Water Resources*, vol. 30, no. 10, pp. 2087–2097, 2007.

[23] H. O. Sharif, D. Yates, R. Roberts, and C. Mueller, "The use of an automated nowcasting system to forecast flash floods in an urban watershed," *Journal of Hydrometeorology*, vol. 7, no. 1, pp. 190–202, 2006.

[24] X. Sun, R. G. Mein, T. D. Keenan, and J. F. Elliott, "Flood estimation using radar and raingauge data," *Journal of Hydrology*, vol. 239, no. 1–4, pp. 4–18, 2000.

[25] W. F. Krajewski, "Cokriging radar-rainfall and rain gage data," *Journal of Geophysical Research: Atmospheres*, vol. 92, no. D8, pp. 9571–9580, 1987.

[26] E. N. Anagnostou, W. F. Krajewski, and J. Smith, "Uncertainty quantification of mean-areal radar-rainfall estimates," *Journal of Atmospheric and Oceanic Technology*, vol. 16, no. 2, pp. 206–215, 1999.

[27] C. Mazzetti and E. Todini, "Combining raingages and radar precipitation measurements using a Bayesian approach," in *Proc. geoENV IV—Geostatistics for Environmental Applications: Proceedings of the Fourth European Conference on Geostatistics for Environmental Applications held in Barcelona, Spain, November 27–29, 2002*, Springer Netherlands, 2004, pp. 401–412.

[28] S. Sinclair and G. Pegram, "Combining radar and rain gauge rainfall estimates using conditional merging," *Atmospheric Science Letters*, vol. 6, no. 1, pp. 19–22, 2005.

[29] T. Wardah, R. Suzana, O. Sazali, A. Hafiz, M. S. Lariyah, and J. Sharmy, "Radar rainfall calibration for improved quantitative precipitation estimates in Kelantan and Terengganu River basins," *International Journal of Civil Engineering and Technology*, vol. 9, no. 8, pp. 27–36, 2018.

[30] W. Tahir, W. H. Azad, N. Husaif, S. Osman, Z. Ibrahim, and S. Ramli, "Climatological calibration of radar ZR relationship for Pahang River basin," *Jurnal Teknologi*, vol. 81, no. 4, pp. 27–33, 2019.

[31] T. J. Kim, H. H. Kwon, and K. B. Kim, "Calibration of the reflectivity-rainfall rate (ZR) relationship using long-term radar reflectivity factor over the entire South Korea region in a Bayesian perspective," *Journal of Hydrology*, vol. 593, 125790, 2021.

[32] K. T. Smith and G. L. Austin, "Nowcasting precipitation—A proposal for a way forward," *Journal of Hydrology*, vol. 239, no. 1–4, pp. 34–45, 2000.

[33] B. W. Golding, "Nimrod: A system for generating automated very short range forecasts," *Meteorological Applications*, vol. 5, no. 1, pp. 1–16, 1998.

[34] N. E. Bowler, C. E. Pierce, and A. W. Seed, "STEPS: A probabilistic precipitation forecasting scheme which merges an extrapolation nowcast with downscaled NWP," *Quarterly Journal of the Royal Meteorological Society: A journal of the atmospheric sciences, applied meteorology and physical oceanography*, vol. 132, no. 620, pp. 2127–2155, 2006.

[35] M. C. Wong, W. K. Wong, and E. S. Lai, "From SWIRLS to RAPIDS: Nowcast applications development in Hong Kong," in *Proc. PWS Workshop on Warnings of Real-Time Hazards by Using Nowcasting Technology*, Sydney, Australia, 9–13 October 2006.

[36] D. J. Yik, Y. W. Sang, N. K. Chang, F. J. Fakaruddin, A. Dindang, and M. H. Abdullah, "Analysis of the cyclonic vortex and evaluation of the performance of the radar integrated nowcasting system (RaINS) during the heavy rainfall episode which caused flooding in Penang, Malaysia on 5 november 2017," *Tropical Cyclone Research and Review*, vol. 7, no. 4, pp. 217–229, 2018.

[37] S. Chumchean, A. Sharma, and A. Seed, "An integrated approach to error correction for real-time radar-rainfall estimation," *Journal of Atmospheric and Oceanic Technology*, vol. 23, no. 1, pp. 67–79, 2006.

[38] Q. Qiu, J. Liu, J. Tian, Y. Jiao, C. Li, W. Wang, and F. Yu, "Evaluation of the radar QPE and rain gauge data merging methods in Northern China," *Remote Sensing*, vol. 12, no. 3, p. 363, 2020.

[39] K. Sok and C. Oeurng, "Application of HEC-HMS model to assess streamflow and water resources availability in Stung Sangker catchment of Mekong'Tonle Sap lake basin in Cambodia," preprints, 2016.
[40] B. G. Tassew, M. A. Belete, and K. Miegel, "Application of HEC-HMS model for flow simulation in the Lake Tana basin: The case of Gilgel Abay catchment, upper Blue Nile basin, Ethiopia," *Hydrology*, vol. 6, no. 1, p. 21, 2019.
[41] F. Daide, R. Afgane, A. Lahrach, A. A. Chaouni, M. Msaddek, and I. Elhasnaoui, "Application of the HEC-HMS hydrological model in the Beht watershed (Morocco)," in *Proc. E3S Web of Conferences*, 2021, vol. 314, 05003, EDP Sciences.
[42] M. J. Fleming and T. Brauer, "Hydrologic modeling system HEC-HMS quick start guide," US Army Corps of Engineers Institute of Water Resources Hydrologic Engineering Center (CEIWR-HEC), CPD-74D, 2016.
[43] S. K. Mishra and V. P. Singh, "Long-term hydrological simulation based on the soil conservation service curve number," *Hydrological Processes*, vol. 18, no. 7, pp. 1291–1313, 2004.
[44] A. N. A. Hamdan, S. Almuktar, and M. Scholz, "Rainfall-runoff modeling using the HEC-HMS model for the Al-Adhaim River catchment, northern Iraq," *Hydrology*, vol. 8, no. 2, p. 58, 2021.
[45] S. Ranjan and V. Singh, "HEC-HMS based rainfall-runoff model for Punpun river basin," *Water Practice & Technology*, vol. 17, no. 5, pp. 986–1001, 2022.
[46] M. U. Nadeem, Z. Waheed, A. M. Ghaffar *et al*., "Application of HEC-HMS for flood forecasting in hazara catchment Pakistan, south Asia," *International Journal of Hydrology*, vol. 6, no. 1, pp. 7–12, 2022.
[47] D. N. Moriasi, J. G. Arnold, M. W. Van Liew, R. L. Bingner, R. D. Harmel, and T. L. Veith, "Model evaluation guidelines for systematic quantification of accuracy in watershed simulations," *Transactions of the ASABE*, vol. 50, no. 3, pp. 885–900, 2007.
[48] A. Bárdossy and G. Pegram, "Combination of radar and daily precipitation data to estimate meaningful sub-daily point precipitation extremes," *Journal of Hydrology*, vol. 544, pp. 397–406, 2017.
[49] A. Zahraei, K. L. Hsu, S. Sorooshian, J. J. Gourley, V. Lakshmanan, Y. Hong, and T. Bellerby, "Quantitative precipitation nowcasting: A Lagrangian pixel-based approach," *Atmospheric Research*, vol. 118, pp. 418–434, 2012.
[50] B. W. Golding, "Nimrod: A system for generating automated very short range forecasts," *Meteorological Applications*, vol. 5, no. 1, pp. 1–16, 1998.
[51] A. R. Ganguly and R. L. Bras, "Distributed quantitative precipitation forecasting using information from radar and numerical weather prediction models," *Journal of Hydrometeorology*, vol. 4, no. 6, pp. 1168–1180, 2003.